The design, control and testing of an integrated electrohydrostatic powered ankle prosthesis

Tian Yu, Andrew Plummer, Pejman Iravani, Jawaad Bhatti, Saeed Zahedi KBE, David Moser,

***Abstract*— This paper presents a prototype powered ankle prosthesis which can operate passively in most of the gait cycle and provide powered assistance for toe push-off and subsequent foot dorsiflexion. The use of electrohydrostatic actuation (EHA) gives the ability to switch quickly and smoothly between passive and active modes. In this new powered ankle prosthesis, the motor-pump unit is integrated with the ankle joint and the battery and controller are held in a backpack. A 100W brushless DC motor is used to drive a 0.45cc/rev gear pump, controlling flow to an ankle cylinder through a bespoke manifold. The motor runs wet, pressurised to 6MPa, avoiding the need for a pump shaft seal and a refeeding circuit for external leakage. A dynamic system model has been develop to help analyse the EHA performance. A motor control method is proposed based on heel strike recognition and a middle stance time delay. The prosthesis has been tested with a 70kg transtibial amputee, and results are presented for walking on a treadmill at three different speeds (2.8, 3.8 and 4.8 km/h). The amputee has provided positive subjective feedback. We conclude that the hybrid passive-active approach has significant advantages for prosthesis design, and we outline future testing and development requirements.**

***Index Terms*—EHA, powered ankle prosthesis, medical robotics**

I. Introduction

PASSIVE spring-based ankle-foot prostheses are now common. They use an elastic structure to absorb the energy in the early stance phase (heel strike) and middle stance phase (dorsiflexion). The stored energy is returned to assist walking in the terminal stance phase (toe-off) [1-3]. This kind of passive spring-based ankle-foot prosthesis can achieve a natural gait to some extent (especially in low speed walking), and has several advantages including low weight, quietness, un-limited range, robustness and relatively low cost. Some more intelligent ankle prostheses are also commercially available. As an example, the Elan foot uses controllable hydraulic damping to offer smooth ankle joint motion, which significantly improves the walking experience of amputees [4]. The Proprio foot has electrical actuation at the ankle joint to adjust the ankle angle, so it can lift the toe in the swing phase to improve ground clearance and assist stand-up [5].

To provide increased functionality for lower limb amputees, researchers are investigating powered ankle prostheses in which power will be used to actively assist walking, particularly at higher speed and up slopes, and for stair climbing. A DC motor with mechanical transmission is a popular actuation technology proposed for ankle prostheses [6-10]. However all ankle movement requires electrical power in these designs, including providing resistance in passive phases. BioM [11] is the first commercially available powered ankle prosthesis which can improve amputee metabolic economy on average by 14% compared with a passive spring based ankle [12] but its power requirement limits walking range, i.e. the ankle cannot provide controllable resistant without driving the motor actively. Pneumatically actuated ankle prostheses are also popular for research [13-15], but they are limited by their power density and controllability in comparison with hydraulic power transmission. Pneumatics gives low power density due to lower pressure (typically below 1MPa, compared to hydraulics which is an order of magnitude higher). Also the higher compressibility of air compared to hydraulic oil (by a factor of about 10000) gives significant delays in power transmission, and makes it difficult to provide smooth motion in the presence of friction [16].

Different control strategies for active lower limb prostheses have been reviewed in [17, 18]. A k-nearest-neighbor algorithm is used to classify the user's intention into standing or three different walking speeds in [19]. [20] proposed using EMG signals are used to switch between level ground walking and stair descend modes. [21] proposed using a preprogramed time-based ankle motion pattern as the actuator position reference. The phase-based control strategy has been adopted for many active and semi-active ankle prostheses [7, 22-27], which is because the ankle kinematic and kinetic characteristics are quasi-periodic and can be categorised into several gait phases. As shown in Fig. 1, the ankle motion in a gait cycle during level walking is divided into early stance phase (heel strike), middle stance phase, terminal stance phase and swing phase. In each phase, the human ankle can be considered as a passive element with fixed stiffness and damping (in the early and middle stance phase) or a power source (in the terminal stance phase and early swing phase). The main problem is then focused on the real time detection of the gait phase or the correct identification of the transitions between phases [18].

The problem being addressed in this paper is the development of an actuation approach which allows extended range by only requiring power input in some phases of the gait cycle, and being able to operate passively in other phases. Developing a control method which is appropriate for such an actuation approach is part of the challenge. The prosthesis should also be able to operate satisfactorily as a passive device if the battery becomes discharged.

Electrohydrostatic actuators (EHAs) are widely used in aerospace, and increasingly used in industrial hydraulics. An

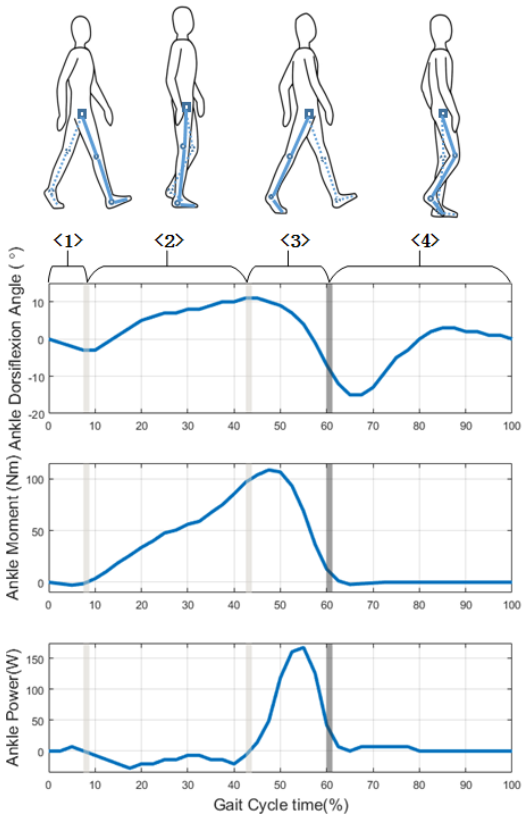

Fig. 1: Human gait decomposition and ankle motion of healthy subjects (70kg) using data from [33]. <1>Early stance phase (heel strike); <2>Middle stance phase; <3>Terminal stance phase (active plantarflexion); <4> Swing phase. The thick dark bar in the figure indicates the toe-off.

EHA consists of a servomotor driven pump directly supplying a hydraulic cylinder. Adding valves in the hydraulic circuit gives a way of easily switching between modes of operation to change behaviour. An EHA can give a high gear ratio between motor and joint, with design freedom for motor location, and has good physical robustness [28], and so is promising for use in lower limb prosthesis applications. [29] proposed using an EHA actuated prosthetic knee which can switch between fully powered and passive damping modes. This semi-active knee prototype is compact (28cm in length) and low weight (4kg) with a battery life to allow at least 3000 steps per day. This ability to switch between active and passive modes is also a key novelty of the prosthetic ankle research reported in [30], but no evidence that a prototype was built has been found. Our earlier work described a powered ankle prosthesis using an off-ankle EHA, i.e. a servomotor and pump in a backpack connected to a cylinder and valves in the ankle. This demonstrated the principle of quickly and smoothly switching between passive and active modes [31]. The EHA was used to assist walking within certain time windows within a gait cycle, specifically the plantarflexion (PF) before toe-off, and dorsiflexion (DF) in the early swing phase for toe-lifting. In the rest of the gait, the actuation system operated passively with controllable damping, which reduced the average power draw and also allowed safe passive prosthetic function after the battery discharged.

The prototype described in [31, 32] has a servomotor and pump arrangement that is too large and heavy for mounting on the ankle, so it has a pair of hydraulic hoses to connect the motor-pump unit in the backpack to the ankle joint. The hydraulic hoses were inconvenient and were found to restrict movement. The new prototype described in this paper is the first compact powered ankle prosthesis which integrates the EHA with the ankle joint. This new prototype can deliver the same level of assistance power with a 2.2kg powered ankle and a 1.1kg battery (still in the backpack with the controller, giving a total backpack weight of 2.3kg).

A timing control method for this EHA powered ankle prosthesis is proposed, which uses foot strain gauge signals to recognise the heel strike and to trigger powered PF assistance after a time delay. This is the first gait controller using foot spring strain gauge signals to detect the phase transfer, since the load difference between the foot and toe spring directly indicates the body weight moving forwards. The middle stance delay before the triggering of powered PF assist gives the potential for adaptation to different walking speeds, although automatic speed adaptation is not included in this paper.

The performance of this prototype and its controller have been validated in a variety of walking tests with a transtibial amputee. The ankle design, control method and some of the amputee trial results are presented in this paper.

II. PROTOTYPE DESIGN

The powered ankle prosthesis prototype is shown in Fig. 2, and its main components and their sizing are summarized in Table. I. The controller and battery are carried in a backpack in this implementation, so are not seen in the figure. The prototype's hydraulic circuit is shown in Fig. 3. The function of each subsystem is described in the following sections, along with bench test results.

A. Motor-pump Unit Integration

An integrated motor-pump unit has been designed in which the pump casing is pressurised to about 6MPa pre-charge pressure. When driven, the pump outlet line will increase in pressure, and the inlet line will drop. The 6MPa pre-charge pressure is sufficient to prevent cavitation at the pump inlet side of the closed circuit without the need for any additional hydraulic circuitry. However, to achieve low friction, standard pump shaft seals will not withstand such a high casing pressure, so no shaft seal is used in this design. Instead fluid is allowed to leak into the chamber containing the servomotor-pump coupling, and into the servomotor body. Thus the permanent magnet rotor in the servomotor runs wet, i.e. in hydraulic oil, and the pump casing, coupling chamber, and servomotor cavity form one interconnected pressure vessel (on the right hand side of Fig. 2(a)). The pressurised fluid in the motor cavity refeeds into the closed circuit via the leakage path of the pump to compensate the oil volume variation in the closed circuit, caused by temperature changes or non-linear oil stiffness. To accommodate these volume changes with minimal change in the pre-charge pressure, a piece of compliant power steering hose is attached to the motor end cap to act like a small accumulator, supplementing the volume in the motor cavity, and is shown as an accumulator symbol in Fig. 3. In summary, the advantage of this arrangement is that without a shaft seal, friction is reduced, and there is no longer a requirement to

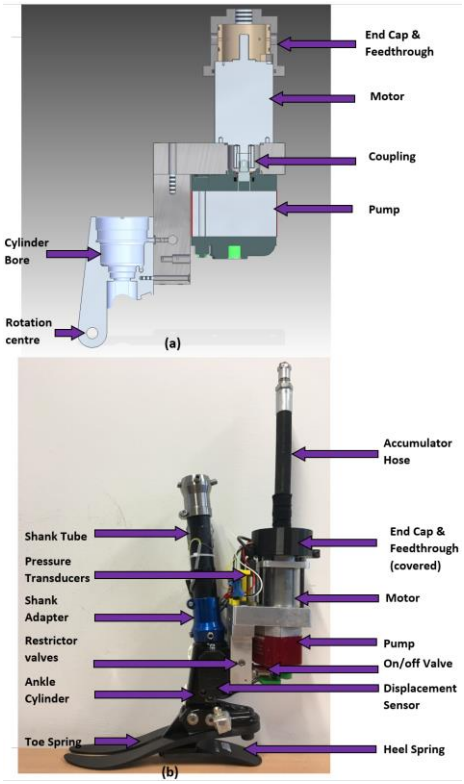

Fig. 2: The EHA powered ankle prosthesis prototype. (a) Cross section of the assembly model. (b) Prosthesis prototype.

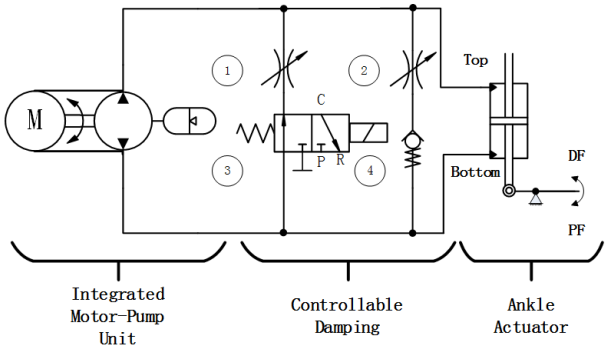

Fig. 3: The hydraulic circuit of the powered ankle prosthesis.

provide a case drain to limit the housing pressure of the pump and then a refeeding circuit to connect the case drain flow back into the closed main circuit. The oil used in this prototype is ISO VG 32.

The motor has a welded steel casing designed to withstand an internal pressure. Since commonly available electrical multi-wire high pressure feedthroughs are too large for this application, a special feedthrough structure has been designed into the motor end cap, comprising a PVC (Polyvinyl Chloride) ring piece as insulator and 8 metal screws (3 for motor power wires and 5 for motor hall effect sensors) as conductors.

B. Controllable Damping

The bypass restriction valves (valve 1&2 in Fig. 3) are from the Echelon foot manufactured by Blatchford [34], and can be manually adjusted to set the damping force in either direction. A 3-way solenoid valve (valve 3 in Fig. 3) is in series with the passive DF restriction valve (valve 1). This 3-way valve works as an on/off valve, which is normally open (from port P to port C) in the passive phase and lets fluid pass through valve 1 in the passive DF phase (mid-stance). In the active PF phase, this on/off valve will be closed (in the position shown in the figure) to avoid flow loss through valve 1. The other bypass restriction valve (valve 2) will pass flow in the passive PF phase (heel strike) and the active DF phase (toe lifting in the swing phase), due to opening of the check valve 4. In the active DF phase, the load on the ankle is not high enough to cause much bypass flow rate across valve 2, thus this bypass line does not need to be fully closed. This operation is summarized in Table. II. Note that although manually adjusted restriction valves are used in the prototype, electrically settable valves are currently used on some commercial ankle prostheses (e.g., [4]), and their use would give the option for automatically changing damping for different conditions (e.g. different walking speeds).

TABLE I
MAIN COMPONENTS IN THE EHA POWERED ANKLE PROSTHESIS PROTOTYPE.

Component	Main Features	
Maxon EC-i 40 High Torque Brushless DC Motor	Nominal Voltage Rated Power Nominal Speed Stall Torque	48 V 100 W 4460 rpm 5.02 Nm
Escon Module 50/5 Servo Controller	Nominal Voltage Maximum Output Current	10-50 V 15 A
Hydraproducts KV0R04RBZZE Reversible Gear Pump	Displacement	0.45 cc/rev
Lee SDBA2531012B 3-way Normally Open Solenoid Valve	Pull-in Voltage Current Drain	12 V 0.4 A
Mountfield MBT4820Li Lithium-Ion Battery	Output Voltage Capacity Weight	48 V 2 Ah 1.1 kg
Blatchford Elan Ankle Joint Cylinder	Actuator Working Area Movement Range	6.28 cm² 21°

C. Ankle Joint Hydraulic Cylinder

The ankle joint hydraulic damper cylinder is adopted from the Elan foot manufactured by Blatchford (enlarged stroke version) [4]. An adapter is used to connect the dome at the top of the cylinder body and the shank tube, as shown in Fig. 2(b). The mounting angle can be tuned by adjusting the adapter screws to achieve a comfortable inversion/eversion angle and utilize the full dorsiflexion/plantarflexion rotation range.

D. Sensors and Electronics

The sensors used in the EHA powered ankle prototype are summarized in Table III. Two pressure transducers are connected at the output ports of the pump to monitor the pressure in the circuit. A magneto-inductive displacement sensor is attached on the ankle cylinder and its target magnet is glued on the foot carriage. The angular position of the ankle joint can be deduced from this displacement measurement. An IMU (Inertial Measurement Unit) is installed on the ankle cylinder body to record the shank orientation. Three strain gauges are attached to the foot spring.

The motor is driven via an Escon Servo Controller (see Table I) in velocity control mode. This uses a proportional-integral based closed loop velocity controller, so the motor drive input

TABLE II
THE OPERATING CONDITIONS FOR DIFFERENT PHASES IN A GAIT CYCLE.

Gait Phase	Heel strike	Middle stance	Terminal stance	Swing	
Ankle Rotation Direction	PF	DF	PF	DF	-
Active/Passive Mode	Passive	Passive	Active	Active	Passive
Cylinder High Pressure Side	Top	Bottom	Bottom	Top	-
Restriction Valve in use	②	①	-	②	-
On/off Valve ③	Open	Open	Closed	Open	Open

Table III
SUMMARY OF THE SENSORS USED IN THE PROTOTYPE.

Sensor	Main Features	
Variohm Pressure Sensor EPT1200-K-1600-B-4-A	Pressure Range	0 ~ 16M Pa
	Accuracy	< +/- 0.8%
Micro- Epsilon Magneto-inductive Displacement Sensor MDS-45-K-SA	Mearing Range	4~24 mm
	Linearity	< +/- 3%
Strain gauges	Resistance	120Ω
Inertial Measurement Unit	Output Signals: 3 axes accelometeres, 3 axes gyroscopes, 3 axes rotation angle	

Table IV
SUMMARY OF THE EHA PERFORMANCE FROM BENCH TEST.

Mechanical output	Pump output	Motor output	Motor input
43 Nm	4.6M Pa	0.558 Nm	6 A
1.344 rad/s	1.01 L/min	272 rad/s	27.13 V
57.8 W	77.7 W	151.8 W	162.8 W

from the high level controller is a motor velocity demand. Actual motor velocity and motor current can be measured. The high level controller is a sequential phase-based method as described in Section IV. Other than using trigger signals from the ankle sensors this high level controller is open-loop.

E. Bench Test

The prototype has been tested in the laboratory to verify the EHA performance. In the bench test, the ankle is driven against a constant load. The test rig has been described in [31]. The result of an example test, in which the EHA was subject to a step change in motor speed demand, is shown in Fig. 4 and summarized in Table. IV. The EHA is running against a constant load of 43Nm, and also some inertia loading as indicated by the peak in pressure difference and motor current (proportional to motor torque) at 0.15s. From about 0.2s to 0.4s the speed, current and pressure difference are roughly constant, consistent with the constant ankle moment loading. The maximum pressure difference and motor current occur just after 0.4s when the piston reaches end-stroke. The performance of this prototype is equivalent to the previous prototype (with off-ankle hydraulic power source, i.e. servomotor/pump in a under the same load condition according to the bench

test results shown in [31]. The subjective amputee test results using this previous prototype indicated that it could provide sufficient power to significantly assist walking for an amputee up to 80kg in weight [32], and so similar assistance capability is expected with the new integrated device. The total efficiency, calculated from the motor electrical input power to the ankle mechanical output power, is only about 36% in this high-load

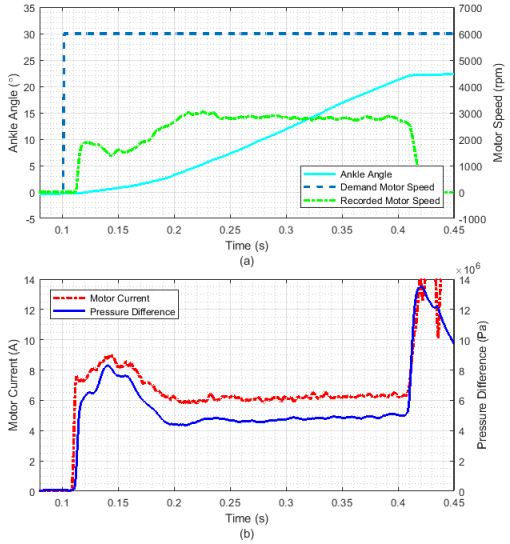

Fig. 4: Bench test result of 43Nm constant load. (a) Ankle PF angle and motor speed. (b) Motor current and pressure difference across pump (subtracting top pressure from bottom pressure).

condition however. In the study in [8], the energy efficiency of the motor with optimal combination of gear box and lead screw is 37%, which is a similar level.

III. SYSTEM MODEL

A simulation model has been developed to help analyse the performance of the EHA. The characteristics of the hydraulic actuation system in both the passive and active phases are modelled.

The hydraulic actuation model is simplified as a symmetric model. The oil compressibility was found to have limited effect on the results, and is not included in the model. The pump flow model is given by:

$$Q_p = D\omega - K_{in}\Delta P_p \quad (1)$$

where D is the pump displacement; ω is the motor-pump angular velocity; Q_p is the pump flow rate; ΔP_p is the pressure difference across the pump; K_{in} is the internal pump leakage coefficient.

The pressure loss in the manifold connecting pump to cylinder was found to be significant. Based on component test results, a linear pressure loss model was adopted:

$$\Delta P_a = \Delta P_p - K_l Q_p \quad (2)$$

where ΔP_a is the pressure difference across the actuator (cylinder), which is also the pressure difference across each bypass restriction valve (valve 1&2 in Fig. 3); K_l is the

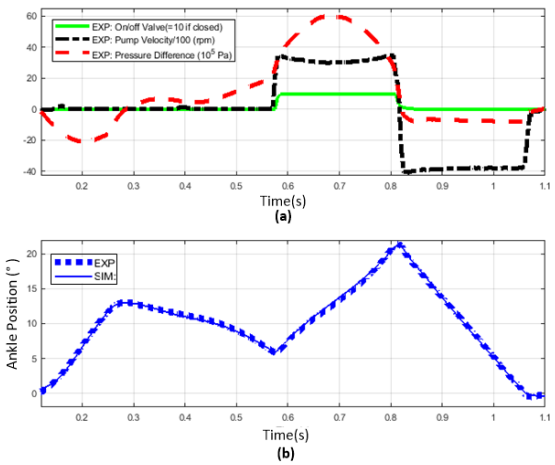

Fig. 5: Comparison between treadmill walk experiment results and the simulation result.

manifold pressure loss coefficient. The bypass restriction valves give a difference between the pump and actuator flows thus:

$$\begin{cases} Q_a = Q_p - K_B\left(K_{bp1}\sqrt{\Delta P_a} + K_{bp2}\Delta P_a\right) & for\ \Delta P_a \geq 0 \\ Q_a = Q_p - \left(-K_{bd1}\sqrt{|\Delta P_a|} + K_{bd2}\Delta P_a\right) & for\ \Delta P_a < 0 \end{cases} \quad (3)$$

where Q_a is the flow rate in/out of the actuator; K_B is the coefficient for on/off valve ($K_B = 1$ if the on/off valve is open and $K_B = 0$ if the on/off valve is closed); K_{bp1} and K_{bp2} are the bypass pressure/flow coefficients for the active PF phase and the passive DF phase (valve 1 in Fig.3 activated), which combines both a square-root and the proportional relationship in the bypass line. K_{bd1} and K_{bd1} are the bypass pressure difference to flow rate coefficients for the active DF phase and the passive PF phase (valve 2 in Fig. 3 activated). The actuator was approximated as a proportional relationship between the actuator flow rate and ankle rotation speed:

$$\dot{\theta} = K_a Q_a A^{-1} \quad (4)$$

where $\dot{\theta}$ is the ankle rotation speed; A is the annular area of the double-ended cylinder; K_a is a lever ratio between the piston rod extension speed and the ankle angular speed.

The results from a treadmill walking experiment have been used to validate the simulation model. In the experiment, a transtibial amputee was walking on a treadmill at a constant speed of 3.8km/h wearing the compact powered ankle prosthesis. The pressure difference across the pump, motor speed and on/off valve current signals shown in the upper graph of Fig. 5 were recorded and were used as the input signals of the simulation model. By matching the simulated ankle angular position with the treadmill walk experiment results, the unknown coefficients in the simulation model were estimated. The comparison between the simulated and experimental ankle angular positions is shown in the bottom graph of Fig.5. The gait starts from heel strike, where a negative pressure pulse causes the passively PF movement of the ankle. The ankle then passively DF with a small damping due to the body weight moving forwards until the powered PF phase is started at about 0.57s. Within the powered PF phase, the motor is demanded to run at maximum speed against the high load and the on/off valve is closed to ensure the full power from the motor is delivered to the ankle actuator. The motor speed demand is reversed to rotate the ankle to the maximum DF position once the powered PF phase is ended. The parameters in the model are summarized in Table V.

TABLE V
SUMMARY OF THE SIMULATION MODEL PARAMETERS

Symbol	Specification	Value
D	Pump Displacement	0.45 cc/rev
K_{in}	Pump Internal Leakage Coefficient	1.46×10^{-12} m³/s/Pa
K_l	Manifold Pressure Loss Coefficient	9×10^{9} Pa/m³/s
K_{bp1}	Active PF Bypass Coefficient 1 (square-root)	4.275×10^{-9} m³/s/Pa
K_{bp2}	Active PF Bypass Coefficient 2 (linear)	1.575×10^{-12} m³/s/Pa
K_{bd1}	Active DF Bypass Coefficient 1 (square-root)	6.75×10^{-8} m³/s/Pa
K_{bd2}	Active DF Bypass Coefficient 2 (linear)	1.1×10^{-11} m³/s/Pa
A	Actuator Annular Area	6.28 cm²
K_a	Ankle Joint Lever Coefficient	2.64 °/mm

As shown in Fig.5, the simulation model can accurately predict the ankle motion under the real load situation in both passive and active phases. More details and validation of the simulation model can be found in [35].

IV. CONTROL METHOD

A. Control Strategy

The quasi-periodic characteristic of the ankle when walking, introduced in Section I, indicates the ankle motion in a gait cycle can be divided into two passive phases with controllable damping and two active phases requiring power assist. In this EHA-powered prosthesis, the phase transition between the heel strike and the middle stance phase and the damping in these two passive phases are controlled by the valves 1 to 4 in Fig.3. The timing of the transition between the middle stance phase and the terminal stance phase (the switching point between passive and active operation mode) is critical to provide a natural walking gait and to make the most use of the power from the EHA. Powering the PF (in the terminal stance phase) too early will result in the ankle lifting the body upwards instead of pushing the body forwards. Powering the PF too late will result in a lack of support of the body weight, which means the amputee will be in danger of stumbling. This power input needs to start a certain time after the body weight switches from the heel to the toe, thus a timing control method is proposed and will be presented in section IV.C.

B. Amputee Trial with Passive Ankle

An amputee trial with the ankle functioning passively was undertaken in order to gather ankle sensor signals to aid controller design. The prosthesis prototype was tested by a 70kg transtibial amputee in the indoor test site at Chas A Blatchford & Sons Ltd., UK. During fitting the mounting angle was adjusted, and the DF and PF restrictor valves were set to meet the damping requirement of the amputee. The amputee has been asked to walk on a treadmill at 14 different speeds from 2.8km/h to 5.4km/h.

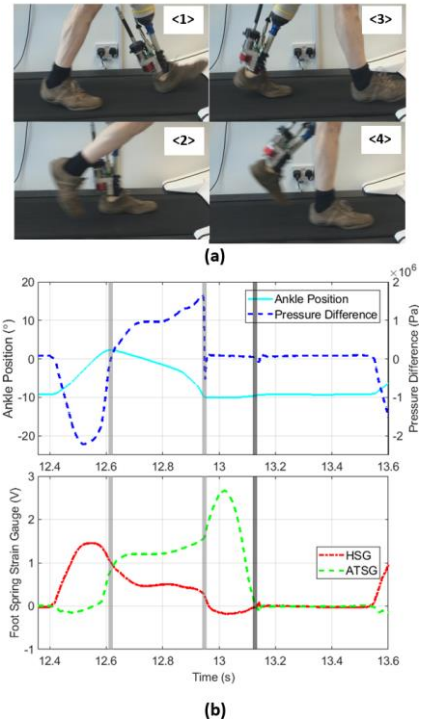

Fig. 6: A typical gait at 3.8km/h walking speed in amputee trial with passive ankle. (a) Different phases in a gait cycle. (b) Ankle angle, pressure difference across pump and foot strain gauge signals.

A typical gait cycle at 3.8km/h treadmill speed is shown in Fig. 6. The ankle starts to passively plantarflex once the heel contacts the ground at the beginning of the heel strike phase (phase <1>). During this phase, a peak pressure difference across the ankle joint cylinder of 2.2MPa occurs, which corresponds to the heel strain gauge (HSG) signal peak (1.45V) in the bottom graph. The grey bar between phase <1> and phase <2> indicates the finish of the heel strike when the ankle PF is a maximum. At the beginning of phase <2>, the HSG signal and the average toe strain gauge (ATSG) signal cross each other, which indicates that the bodyweight is moving forward. The grey bar between phase <2> and phase <3> indicates the time point of maximum ankle DF. Due to the lack of powered PF movement in the terminal stance phase, the ankle joint keeps the maximum DF position until the start of the next gait. The ATSG signal keeps increasing in phase <2> and peaks at 2.65V in phase <3> after the ankle piston reaches the end stroke. Phase <4> is the swing phase and the dark grey bar between phase <3> and phase <4> indicates the toe-off.

As shown in Fig. 6, the heel strike has unique features which could be used to recognise the walking intention of the amputee and to demarcate the start of a gait cycle. The peak of the HSG signal in particular clearly shows the impact on the heel. The powered PF assist should be started when most of the body weight is moved to the toe spring at the end of the middle stance phase, which could be triggered by a time delay after the HSG signal crosses the ATSG signal.

C. Timing control method

A timing control method for the EHA powered ankle prosthesis is proposed, which is based on heel strike recognition and a middle stance time delay. Based on the passive patient trial results, the heel strike can be recognised using the differential signal between HSG and ATSG (HSG-ATSG). As shown in Fig. 7, the impact on the heel (signal peak of HSG-ATSG) is recognised by setting two detection points. The first detection point is when the HSG-ATSG signal crosses a pre-set threshold 1 upwards (the minimum heel load value in passive walking) and the second detection point is when the HSG-ATSG signal crosses a pre-set threshold 2 downwards, i.e. the load has been switched to the toe. When the heel strike is recognised by the control program, the powered PF assist is triggered after a customized time delay which can be adjusted to fit different walking speeds. Note that the passive test results provide the broad signal characteristics, but all parameter values are determined in active walking tests.

To avoid falsely triggering the powered PF assist by other movements, the heel strike recognition is completed by the combination of the HSG signal, HSG-ATSG signal and the detection duration. The control algorithm is shown in Fig. 8, in which the rectangle symbols indicate different phases and the diamond symbols indicate decisions, and in this case thresholds 1 and 2 are set to 1V and 0V respectively. The decision {1} and {2, 3} in Fig. 8 are equivalent to the detection point 1 and 2 in Fig. 7. At detection point 2 (decision {3} in Fig.8), the HSG is required to be higher than a certain value, the heel load value (0.5V) measured in double stance, to make sure the heel is on the ground, which can prevent a false trigger caused by stamping on the prosthetic heel. If the heel strike recognition stage (decision {4} in Fig.8) is too long, it indicates that the amputee may not be walking, e.g. they may be standing on the prosthetic foot alone or swaying the body between heel and toe. The threshold selection and the control algorithm are discussed in more detail in [35].

The control program is implemented using Labview and is run on a cRIO (compact Real-time Input/Output processor). The sample rate is 200Hz, which gives about 50 readings in the heel strike and middle stance phase respectively. The high sample rate is important since the amputee is very sensitive to the start time of the powered PF. According to the feedback of the amputees who took part in the patient trial of the earlier prototype described in [32], a 5ms variation is just distinguishable by the amputee.

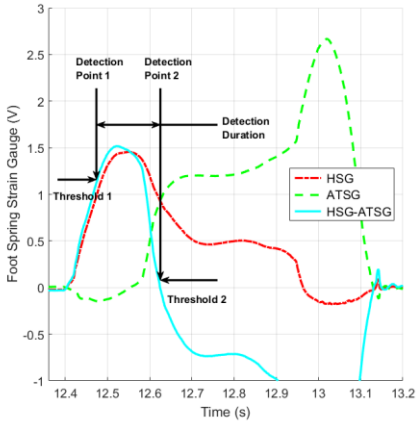

Fig. 7: Detection points of heel strike recognition.

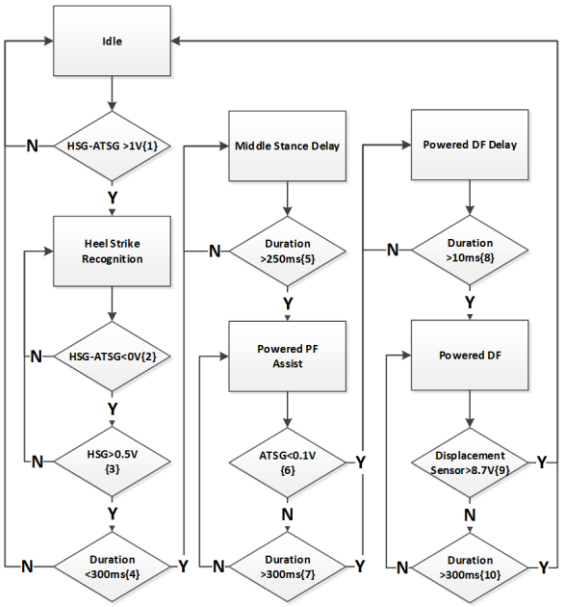

Fig. 8: Control algorithm flow chart.

The motor's servo controller is set up in closed loop speed control mode with PI controller. Within the powered PF phase, the controller steps the motor speed demand to a maximum (6000rpm). The unloaded motor response to a 6000rpm demand step exhibits a 2ms delay and 1ms time constant [35], giving an estimated -3dB bandwidth of 160Hz. The motor is stopped by the control program when the ATSG drops below a small value (decision {6} in Fig.8), thus the PF is powered until the toe spring nearly leaves the ground. The motor will also be shut down if the duration of the powered PF phase exceeds a certain duration (decision {7} in Fig.8) to protect the motor and the amputee. After a short delay (decision {8} in Fig.8), the motor demand reverses direction and dorsiflexes the ankle to the maximum DF position (decision {9} in Fig.8) to clear the ground.

V. Powered Ankle Amputee Trial

A. Amputee Trial Set up

The EHA powered ankle prosthesis prototype has been tested by a 70kg transtibial amputee in the indoor and outdoor test sites at Chas A Blatchford & Sons Ltd. (the same amputee as in the passive trial). The pre-test mounting and adjustment process is the same as that described in section IV-B. A 2Ah, 1.1kg lithium-ion battery [36], the cRIO and other electronics were held in a backpack and carried by the amputee. The amputee walked on a treadmill at three different speeds: slow speed at 2.8km/h; medium speed at 3.8km/h and high speed at 4.8km/h, which were selected according to the daily walking speed range of the amputee. The amputee also walked outside on a slight upslope at a self-selected speed [37].

The ankle rotation angle α (recorded by the displacement sensor) and the shank rotation angle β (recorded by the IMU) are defined as shown in Fig. 9. When the amputee is standing as shown in Fig.9(a), the ankle angle is at 0° and the IMU coordinate frame x′, y′, z′ is approximately aligned with the

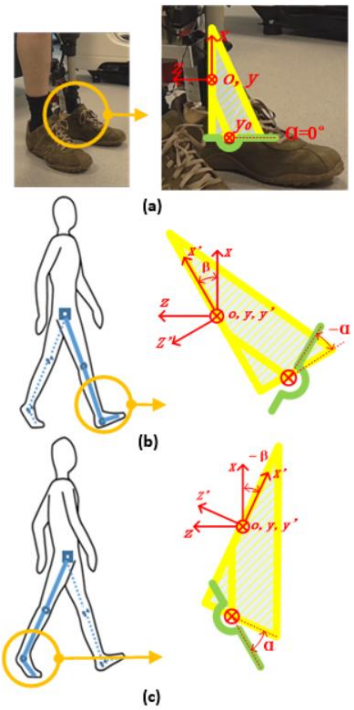

Fig. 9: The rotation of the shank when standing and walking. (a) Coordinate frame at stand-still. (b) Ankle and shank angles when the shank-ankle is in front of the torso. (c) Ankle and shank angles when the shank-ankle is behind the torso.

reference frame x, y, z. When the amputee is walking, the shank is mainly rotating around the axis y, which is parallel to the initial ankle joint axis y0, and the rotations around the axes x and z are neglectable. Fig. 9(b) shows the status at the beginning of the stance phase of a gait cycle, when the shank-ankle is in front of the torso. In this position, the shank rotation angle β is at the maximum value and the ankle rotation angle α is at the maximum DF angle. Fig. 9(c) shows the status at the end of the stance phase, when the shank-ankle is behind the torso. In this position, the shank rotation angle β is negative and the ankle rotation angle α is at approximately the maximum PF angle.

B. EHA Performance and Timing Control

Measurements from a typical gait cycle in the amputee trial are shown in Fig 10, taken from a treadmill test at 3.8km/h. The gait cycle starts from the heel strike and the gait duration is 1.155s. The first grey bar at about 17% of the gait cycle indicates the transition between the heel strike and the middle stance phase. The second grey bar at 40% of the gait cycle indicates the start of the powered PF phase. The third grey bar at 60% of the gait cycle indicates the end of the powered PF phase when the toe is leaving the ground.

A comparison between ankle angle and shank angle is shown in Fig. 10(a). At the start of the heel strike, the ankle is at the maximum DF position and the shank angle is also at a maximum. The ankle rotation direction in each stance phase is consistent with Table. II, and the full 21° range of motion (RoM) of the ankle prosthesis is used. The shank is rotating in a single direction in the stance phase. After the toe leaves the ground at 60% of the gait cycle, the shank is still rotating in the same direction until 72% of the gait cycle. The foot is lifted by

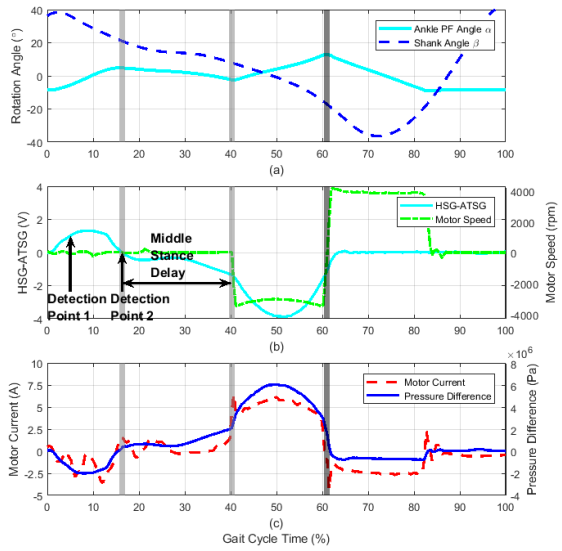

Fig. 10: Typical gait cycle from 3.8km/h treadmill walking. (a) Ankle and shank angle. (b) Motor speed and HSG-ATSG signal. (c) Motor current and pressure difference.

the upper joints (knee and hip) during swing. When the shank angle crosses zero at about 87% of the gait cycle, the shank tube is vertical, and the foot is closest to the ground. The toe should be lifted (DF) before this time to clear the ground.

The strain gauge signal difference between the heel spring and the toe springs (HSG-ATSG), which is the main signal used to recognise heel strike and to trigger the powered PF assist, is shown in Fig. 10(b). The HSG-ATSG signal crosses the first threshold (1V) at about 55ms (detection point 1) and crosses the second threshold (0V) at about 200ms (detection point 2). Hence the heel strike is recognized by the control program and the powered PF assist is started after the middle stance time delay. The middle stance delay times for different walking speeds are pre-set according to the amputee's feedback and are 340ms for 2.8km/h; 250ms for 3.8km/h and 230ms for 4.8km/h. In each case these values could be found by trial and error over about 1 minute of walking.

The recorded motor velocity is shown in Fig. 10(b) and motor current and pressure difference across the pump are shown in Fig. 10(c). Due to the heel strike, a 2MPa pressure difference across the pump is seen at 10% gait cycle time. Since the motor speed demand is zero in the heel strike and middle stance phase, a motor current is needed to hold the motor against the load pressure difference, peaking at -3A during heel strike and 1.5A at the beginning of the middle stance phase.

The motor current peaks at the beginning of the powered PF phase to accelerate the motor. The motor is accelerated to 3300rpm in 1% of the gait cycle, i.e. the EHA is quickly switched into active mode. Within this powered PF phase, the mean velocity of the motor is 3100rpm driving against the peak pressure difference of 6MPa and the peak motor current is 6A. The powered PF assist duration is 250ms. After the toe spring leaves the ground (indicated by an ATSG signal lower than 0.1V) at 60% of the gait, the motor reverses rotation direction to dorsiflex the ankle. In the powered DF phase, the motor is running at approximately 4000rpm for 200ms and the load pressure across pump is 7×10^5Pa.

C. Ankle Motion Comparison with Healthy Subject

A comparison of the ankle motion between the transtibial amputee and a healthy subject is shown in Fig. 11. The healthy subject data is from [33]. There are 6 overlapping amputee gaits plotted in the Fig.11(a) and (b). The gait cycle starts from the heel strike and the gait duration is 1.140+/-0.015s. As shown in Fig.11(a), the ankle plantarflexes from -8.5° to 5° during heel strike. As the ankle prosthesis has been dorsiflexed to the maximum DF angle in the previous gait and due to the imperfect cushion effect of the heel, the amputee ankle PF angle change during heel strike is much bigger than for a healthy subject. The DF range of the ankle in the middle stance phase is about 7° for the transtibial amputee, which is about half of a healthy subject. In the powered PF phase (22% of the gait cycle between the two grey bars), the ankle has been actively plantarflexed to the maximum 13° in about 250ms. It takes another 200ms to actively dorsiflex the ankle to the maximum DF position. Compared to the healthy subject, the available ankle rotation range for the amputee is slightly smaller. However the rotation range is not fully used in the middle stance phase. In the swing phase, the ankle prosthesis over-dorsiflexes the ankle to the maximum DF position which causes a small amount of energy to be wasted.

Using a small angle approximation, the ankle torque T_{an} in the middle graph of Fig. 11 is estimated from:

$$T_{an} = \Delta P A_a L_a \tag{5}$$

where ΔP is the pressure difference across the pump; A_a is the annulus area of the double acting cylinder; and L_a is the arm length between the cylinder rod and the ankle joint axis.

Since the pressure loss through the hydraulic manifold and the friction in the actuator cylinder are not included in the calculation, the ankle output torque is approximate. In the heel strike phase, the prosthetic ankle provides a 20Nm resistance torque instead of zero for a healthy subject. The ankle torque keeps on increasing in the middle stance phase until the start of

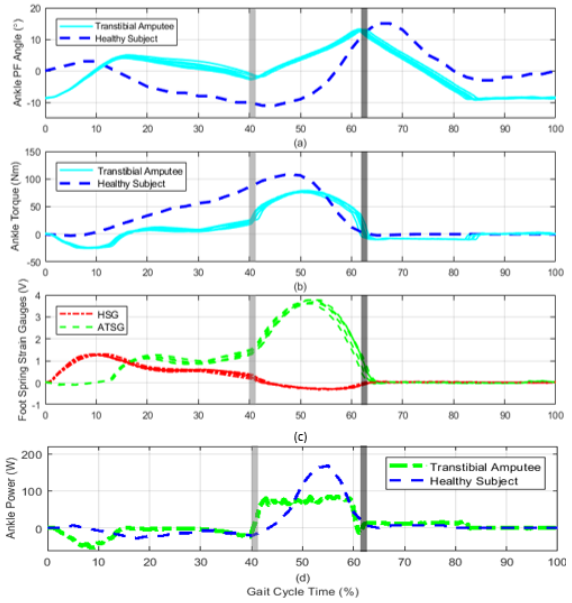

Fig. 11: Ankle motion compared with a healthy subject in a 3.8km/h gait cycle. Healthy subject data is from [33].(a) Ankle PF angle comparison. (b) Ankle torque comparison. (c) Foot spring strain gauge signals. (d) Ankle power comparison.

the powered PF assist, but is only 1/4 of the ankle torque of a 70kg healthy subject. The peak torque provided by the EHA (80Nm at 50% of the gait cycle) during the powered PF is smaller and later than the peak torque of a healthy ankle (110Nm at 47% of the gait cycle). For a healthy subject, the ankle torque is quickly released in the second half of the terminal stance phase, which results in the high speed ankle rotation at the end of the stance phase. However, for the transtibial amputee with the prosthetic ankle, the ankle torque remains over 40Nm in the majority of the powered PF phase. A probable reason is that the function of the upper joint (knee or hip) is altered by the weight of the ankle prosthesis.

The HSG and ATSG signals shown in Fig.11(c) clearly show the switch of the body weight from the heel to the toe. The HSG signal peaks at 1.2V in the heel strike and drops crossing the ATSG signal at about 18% of the gait. After the powered PF assist starts, the ATSG signal increases and peaks at 3.8V. The HSG is negative in the powered PF phase since the toe springs are supporting all the body weight and the heel is affected by the stretch of the shoe.

The ankle output power P_a is calculated from:

$$P_a = \omega_a T_{an} \quad (6)$$

where ω_a is the ankle rotation speed, which is obtained by differentiating the ankle angular position. In Fig.11(d), the negative ankle output power in the passive phase, which peaks at -50 W, shows that power is dissipated by the bypass valves. For the healthy ankle, the heel strike is mainly absorbed by the cushion effect of the heel and the ankle is passively dorsiflexed when the human body is pushed forwards by the other leg in the middle stance phase. Unlike the ankle power of a70 kg healthy subject which peaks at 168W at the end of the terminal stance phase [33], the prosthetic ankle output power remains within 60~85 W. Although the peak ankle power is not achieved, the mean power in the terminal stance phase is approximately the same as the healthy ankle, and the effect of the foot spring means the timing of the two powers is not directly comparable. In the powered DF phase, the ankle output power is similar to the healthy subject.

D. Ankle Motion at Different Walking Speed

Comparisons of the gait duration, heel strike features, powered PF features and shank rotation angle between different walking speeds are summarized in Table. VI. Mean values for 30 steps are given at each walking speed, with standard deviations in brackets. The gait durations can be contrasted with 1.11+/-0.05s for a healthy subject when walking on the level [33]. Compared with the results in [35], the gait duration with the powered ankle is about 0.05s longer than the passive ankle test at each treadmill walking speed.

When the amputee is walking at high speed (4.8km/h), the peak strain gauge signal and peak pressure difference at heel strike is much higher and the heel strike duration is smaller compared to low speed walking (2.8km/h), which indicates that the heel strike impact is more acute when the walking speed is higher. These heel strike features at different walking speeds could be used for real-time walking speed detection.

The powered PF duration is approximately the same between different walking speeds. The peak ATSG and the peak pressure difference in the powered PF phase shown in Table. VI indicates that the ankle torque requirements increase along with the increment in walking speed. The average motor velocity is reduced slightly by the higher load pressure difference in high speed walking.

The maximum shank rotation angle, which occurs at the beginning of the heel strike, is bigger at higher walking speed. This could be used for real-time walking speed detecting. The minimum shank rotation angle did not show clear variation with the walking speed.

E. Subjective Feedback from the Amputee

Both the controller settings and the amputee test set-up are highly reliant on the subjective feedback from the transtibial amputee who took part in the tests, including middle stance delay time at different walking speeds, trigger thresholds, restriction valve settings, treadmill walking test speed range and ankle-shank adapter mounting angle. The feedback from the amputee also helped to evaluate the performance of the powered ankle prosthesis. Some of the comments from the amputee are summarized below.

As shown in Fig. 11, the characteristic of the ankle motion in the powered PF phase is different from the ankle motion of a healthy subject. But according to the amputee, he received sufficient assistance from the powered ankle prosthesis. Without the powered ankle prosthesis, it is difficult for him to attain a high walking speed (4.8 km/h) [37]. In the low speed walking test (2.8 km/h), the amputee suggested the injected power could be reduced for a more comfortable walking experience. The amputee perceived that, with the timing control described, the powered ankle prosthesis consistently pushed him forward instead of lifting him up, and provided good walking assistance [37]. The amputee also stated that the gait with the powered ankle prosthesis felt very natural, and that the prosthetic ankle behaved like the healthy ankle.

TABLE VI
COMPARISON OF THE ANKLE MOTION FEATURES BETWEEN DIFFERENT WALKING SPEEDS.

Walking Speed (km/h)		2.8	3.8	4.8
Gait Duration (s)		1.305(0.028)	1.156(0.033)	1.057(0.013)
Heel Strike Duration (s)		0.188(0.007)	0.164(0.010)	0.135(0.005)
Peak HSG in Heel Strike (V)		0.998(0.066)	1.277(0.112)	1.618(0.109)
Peak Pressure Difference in Heel Strike (10^5Pa)		15.51(1.28)	20.08(2.07)	28.44(2.00)
Powered PF Duration (s)		0.245(0.021)	0.249(0.021)	0.240(0.018)
Peak ATSG in Powered PF (V)		3.294(0.104)	3.717(0.086)	4.012(0.070)
Peak Pressure Difference in Powered PF (10^5Pa)		55.13(1.39)	61.50(1.60)	62.83(0.91)
Average Motor Velocity (rpm)		3050(53)	2977(55)	2907(55)
Shank Rotation Angle, β (°)	Maximum	34.7 (1.48)	38.3 (2.33)	47.5 (1.29)
	Minimum	-36.2 (1.29)	-37.5 (1.65)	-35.2 (1.26)
	Range	70.9 (2.05)	75.9 (2.74)	82.7 (1.07)

The values in this table are given as Mean (standard deviation).

F. Battery Capacity Discussion

Several assumptions can be made to estimate the battery life: the amputee is walking on level ground at a middle speed, around 3.8km/h; the majority of the power is consumed in the powered PF phase. The power consumption in the other phases in a gait cycle is neglectable; the power consumed by the controller and sensors can also be neglected.

From the amputee trial results shown in Fig. 10(c), the average motor current is about 5.2A during the 250ms powered PF phase. So the charge consumption for one step is 1.3As. Thus the 2Ah lithium-ion battery [36] used in this prototype is able to power over 5500 steps, which satisfies the average 3063±1893 steps per day of a lower-limb amputee during typical daily activity [38]. Note that at 48V the 1.3As charge per step is equal to an energy of 63J, which is fairly similar energy consumption as the motor with mechanical transmission (53J/step) reported in [8].

VI. Conclusions & Discussion

This research has investigated a novel electrohydrostatically actuated ankle prosthesis. An important new feature of the EHA system is that it can quickly and smoothly switch between active and passive modes. Thus, the ankle prosthesis can operate passively with controllable damping through some parts of the gait cycle, and can assist walking by driving the ankle in other parts of the cycle, i.e. the powered plantarflexion in the terminal-stance phase (toe push-off) and toe-lifting in the early swing phase to avoid tripping. Compared to powered prosthetic ankles which use a DC motor and mechanical transmission, the ability to provide the desired energy absorption characteristics when required via a well-proven hydraulic damping approach is an advantage. Also, this ankle prosthesis can still operate well purely passively after the battery is drained, which is not possible using most of the other actuation solutions.

The powered ankle prosthesis prototype has the EHA integrated at the ankle joint and weighs 2.2kg. The range of motion of the ankle is 21°, and is capable of 80 Nm output torque in the amputee tests. A timing control method based on heel strike detection and a middle stance time delay is proposed. Foot strain gauge signals are used to recognize the heel strike and trigger the powered PF phase.

The prosthesis and its controller have been tested by a 70kg transtibial amputee. In the amputee trial, the heel strike is correctly recognised by the controller, and by adjusting the time delay according to walking speed the powered PF assist can be triggered at the correct time. Currently the gait controller used in the amputee trial cannot adapt to different speeds, so manual tuning is required. The characteristics at three different walking speeds (2.8, 3.8 and 4.8 km/h) are analysed in this paper. According to the feedback from the amputee, sufficient power assist was provided by the ankle prosthesis and the gait felt very natural. An off-ankle 2 Ah, 1.1 kg lithium-ion battery was used as the power source in the amputee trial, which is estimated to be sufficient to power 5500 steps.

Further controller development is currently ongoing, including varying the input power level for different walking speeds, and powered PF assist trigger timing control based on other sensor signals, so that foot springs can be changed without the need for strain gauging. For example, timing control is being investigated using the ankle/shank motion in the swing phase to calculate walking speed and then adapt the middle stance delay time length to different walking speeds. It is critical to avoid false triggering of powered walking assist as this has the potential to cause a fall, or incorrect timing could cause hyperextension of the knee. Any uncertainty of the triggering of power will reduce the amputee's confidence. Further mechanical integration is also underway to reduce weight and size, making use of novel additive manufacturing methods.

Future amputee trials should involve multiple subjects, including amputees of different weights, heights, levels of amputation (transfemoral or transtibial) and walking habits to further test the performance of the EHA powered ankle prosthesis and its controller.

Acknowledgment

We thank Chas A Blatchford & Sons Ltd., the University of Bath, and the UK Higher Education Innovation Fund for supporting this research.

References

[1] Chas A Blatchford and Sons Ltd. (2016). *Prosthetic Feet* [Online]. Available: http://www.blatchford.co.uk/endolite/category/feet/

[2] Ottobock. (2016). *1C60 Triton* [Online]. Available: http://www.ottobock.com/cps/rde/xchg/ob_com_en/hs.xsl/38138.html

[3] Össur. (2016). *Prosthetic-Solutions/ Feet* [Online]. Available: http://www.ossur.com/prosthetic-solutions/products/all-products/feet

[4] Chas A Blatchford and Sons Ltd. (2016). *élan* [Online]. Available: http://www.endolite.co.uk/products/elan

[5] Össur. (2016). *PROPRIO FOOT®* [Online]. Available: http://www.ossur.co.uk/prosthetic-solutions/products/feet/bionic-feet/proprio-foot

[6] H. M. Herr and A. M. Grabowski, "Bionic ankle–foot prosthesis normalizes walking gait for persons with leg amputation," *Proceedings of The Royal Society B*, vol. 279, pp. 457-464, 2012.

[7] F. Sup et al., "Preliminary Evaluations of a Self-Contained Anthropomorphic Transfemoral Prosthesis," *IEEE/ASME TRANSACTIONS ON MECHATRONICS*, vol. 14, no. 6, pp. 667-676, 2009.

[8] J.K. Hitt et al., "An Active Foot-Ankle Prosthesis with Biomechanical Energy Regeneration," Journal of Medical Devices, vol. 4, pp. 011003-1-9, Mar. 2010.

[9] K. Yuan et al., "Energy-Efficient Braking Torque Control of Robotic Transtibial Prosthesis," *IEEE/ASME TRANSACTIONS ON MECHATRONICS*, vol. pp, no. 99, pp. 149-160, 2016.

[10] Y. Feng and Q. Wang, "Energy-Efficient Braking Torque Control of Robotic Transtibial Prosthesis," *IEEE/ASME TRANSACTIONS ON MECHATRONICS*, vol. pp, no. 99, pp. 1-1, 2017.

[11] BiOM. (2016). *BiOM® T2 System* [Online]. Available: http://www.biom.com/prosthetists/personal-bionics/

[12] S. K. Au et al., "Powered Ankle–Foot Prosthesis Improves Walking Metabolic Economy," *IEEE TRANSACTIONS ON ROBOTICS*, vol. 25, no. 1, pp. 51-66, 2009.

[13] F. Sup et al., "Design and Control of an Active Electrical Knee and Ankle Prosthesis," in *Proc. Of the 2nd Biennial IEEE/RAS-EMBS Int. Conf. on Biomedical Robotics and Biomechatronics*, Scottsdale, AZ, USA, 2008.

[14] R. Versluys et al., "A Pneumatically Powered Below-Knee Prosthesis: Design Specifications and First Experiments with an Amputee," in *Proc. Of the 2nd Biennial IEEE/RAS-EMBS Int. Conf. on Biomedical Robotics and Biomechatronics*, Scottsdale, AZ, USA, 2008.

[15] H. Zheng and X. Shen, "Design and Control of a Pneumatically Actuated Transtibial Prosthesis," *Journal of Bionic Engineering*, vol. 12, no. 2, pp. 217-226, 2015.
[16] D. McCloy and H.R. Martin, *CONTROL OF FLUID POWER: Analysis and Design, 2nd ed*. England:Ellis Horwood Limited,1980.M.
[17] Tucker et al., "Control Strategies for Active Lower Extremity Prosthetics and Orthotics: A Review," *Journal of Neuro Engineering and Rehabilitation*, vol. 12, No.1, 2015.
[18] R. Jiménez-Fabián and O. Verlinden, "Review of control algorithms for robotic ankle systems in lower-limb orthoses, prostheses, and exoskeletons," *Medical Engineering & Physics*, vol. 34, no. 4, pp. 397-408, 2012.
[19] H. A. Varol et al., "Real-time gait mode intent recognition of a powered knee and ankle prosthesis for standing and walking," *in Proc. Of the 2nd Biennial IEEE/RAS-EMBS Int. Conf. on Biomedical Robotics and Biomechatronics*, Scottsdale, AZ, USA, 2008.
[20] S. K. Au et al., "Powered ankle–foot prosthesis to assist level-ground and stair descent gaits," *Neural Networks*, vol. 21, no. 4, pp. 654-66, 2008.
[21] J. K. Hitt et al., "Dynamically Controlled Ankle-Foot Orthosis (DCO) With Regenerative Kinetics: Incrementally Attaining User Portability," in *2007 IEEE Int. Conf. on Robotics and Automation*, Roma, Italy, 2007.
[22] S. K. Au et al., "Powered Ankle–Foot Prosthesis Improves Walking Metabolic Economy," *IEEE TRANSACTIONS ON ROBOTICS*, vol. 25, no. 1, pp. 51-66, 2009.
[23] K. A. Shorter et al., "Technologies for powered ankle-foot orthotic systems: Possibilities and challenges.," *IEEE/ASME Transactions on Mechatronics*, vol. 18, no. 1, pp. 337-347, 2013.
[24] H. M. Herr and A. Wilkenfeld, "User-adaptive control of a magnetorheological prosthetic knee," *Industrial Robot: An International Journal*, vol. 30, no. 1, pp. 42-55, 2003.
[25] R. Kobetic et al., "Development of hybrid orthosis for standing, walking, and stair climbing after spinal cord injury," *Journal of Rehabilitation Research & Development*, vol. 46, no. 3, pp. 447-462, 2009.
[26] Y. D. Li and E. T. Hsiao-Wecksler, "Gait Mode Recognition and Control for a Portable-Powered Ankle-Foot Orthosis," in *2013 IEEE Int. Conf. on Rehabilitation Robotics*, Seattle, Washington, USA, 2013.
[27] F. Zhang et al., "Effects of Locomotion Mode Recognition Errors on Volitional Control of Powered Above-Knee Prostheses," *Ieee Transactions On Neural Systems And Rehabilitation Engineering*, vol. 23, no. 1, pp. 64-72, 2015.
[28] J. J. Charrier and A. Kulshreshtha, "Electric actuation for flight & engine control system: evolution, current trends & future challenges," *45th AIAA Aerospace Science Meeting and Exhibit*, Rano, 2007.
[29] B. Lambrecht and H. Kazerooni, "Design of a Semi-Active Knee Prosthesis," in *2009 IEEE Int. Conf. on Robotics and Automation*, Kobe, Japan, 2009.
[30] M. V. Pillai, "Design of a Semi-Active Knee-Ankle Prosthesis," in *2011 IEEE Int. Conf. on Robotics and Automation*, Shanghai, China, 2011.
[31] T. Yu et al., "The Design of a Powered Ankle Prosthesis with Electrohydrostatic Actuation," in *Proc. Of the ASME/BATH 2015 Symposium on Fluid Power*, Chicago, Illinois, USA, 2015.
[32] T. Yu et al., "Testing an Electrohydrostatic Powered Ankle Prosthesis with Transtibial and Transfemoral Amputees," in *Proc. Of the 7th IFAC Symposium on Mechatronic Systems*, Loughborough, UK, 2016.
[33] R. Riener et al., "Stair ascent and descent at different inclinations," *Gait & posture*, vol. 15, No.1, pp. 32-44, 2002.
[34] Chas A Blatchford and Sons Ltd. (2016). *Echelon* [Online]. Available: http://www.blatchford.co.uk/endolite/echelon/
[35] Tian Yu, "Actuation and Control of Lower Limb Prostheses," Ph.D. dissertation, Dept. Mech. Eng., Univ of Bath., Bath, UK, 2017.
[36] Mountfield. (2017). *MBT4820Li 2.0Ah Lithium-Ion Battery* [Online]. Available: https://www.mountfieldlawnmowers.co.uk/products/freedom48-cordless/mbt4820li-2ah-lithium-ion-battery
[37] Amputee Trial with Powered Ankle Prosthesis Video. (2017). [Electric material provided with manuscript] Basingstoke, UK: Tian Yu.
[38] J. M. Stepien, S. Cavenett, L. Taylor, and M. Crotty, ''Activity levels among lower-limb amputees: Self-report versus step activity monitor,'' *Arch. Phys. Med. Rehabil.*, vol. 88, no. 7, pp. 896–900, 2007.

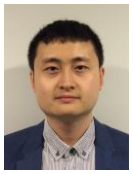

Tian Yu received the B.E. degree in mechanical engineering from Northwestern Polytechnical University, China in 2012, the M.S. degree in fluid power engineering in 2013 from the University of Bath, UK, and a Ph.D from the University of Bath on actuation and control of lower limb prostheses in 2017. His current research interests include fluid transmission, electrohydrulic control and rehabilitation robots.

Professor Andrew Plummer received his Ph.D from the University of Bath in 1991, and worked as a research engineer for Thales from 1990, developing flight simulator control technology, before joining the University of Leeds in 1994. From 1999 until 2006 he was global control systems R&D manager for Instron, manufacturers of materials and structural testing systems. He is now Director of the Centre for Power Transmission and Motion Control, University of Bath, and has published 180 papers in the field of motion and force control, many relating to electro-hydraulic servo-systems.

Pejman Iravani is a robotics lecturer and heads the robotics lab at the University of Bath. His research interests are in computer vision, machine learning, and legged locomotion. He received his PhD in 2005 on a machine learning architecture for collaborative robots.

Jawaad Bhatti is a mechatronics research engineer with the Blatchford Group developing microprocessor controlled lower limb prosthetics and orthotics. He completed his PhD at the University of Bath on the height and step length control of legged robots with springy legs.

Sir Saeed Zahedi KBE FREng FIMechE RDI, Technical Director of Chas A Blatchford & Sons, received the British Health Trade Association life time achievement award for nearly 40 years of service in prosthetics & orthotics in 2013, as well as many other industrial and scientific awards. He is Chair of UK International Society of Prosthetics and Orthotics and is author of over 125 scientific papers and 35 patents. He leads Blatchford's R&D team looking at future integrated products and services in the prosthetics & orthotics field.

David Moser is Head of Research for the Blatchford Group and is also a visiting academic at the University of Southampton. His innovations include the first hydraulic and microprocessor controlled ankles and more recently the "Linx", the first integrated microprocessor knee-ankle prosthesis, the 2016 winner of the prestigious RAEng McRoberts award for engineering innovation. He is author of over 80 peer review journal papers, book chapters and patents in the field of prosthetic, robotics and rehabilitation engineering.